Spectral analysis of near threshold random lasers

R.C. Polson and Z.V. Vardeny
Department of Physics & Astronomy, University of Utah, Salt Lake City, UT 84112

electronic address: rpolson@physics.utah.edu

Abstract

Emission spectra from random lasing systems typically have numerous narrow resonant lines. When excited very near to the laser threshold there are fewer resonant lines which clarify the emission spectrum analysis. We studied three different random lasing systems including π-conjugated polymer films, zinc oxide and TiO2 scatterers in dye solution. Fourier transform analysis of the laser emission spectra near threshold of each system shows that all the sharp lines are highly correlated, indicating that they originate from a single high symmetry resonant structure. The naturally formed microresonators have a circular geometry in the two-dimensional films, and transient spherical geometry in the scatterers/dye suspension.

Highlights

- Near threshold random lasing spectra are based on circles or spheres.
- The Fourier transform provides information to assign the emission peaks.
- The same analysis works for multiple random lasing systems.

Keywords: random lasing, Fourier transform, microresonator

1. INTRODUCTION

Disordered optical gain systems that produce laser emission with sharp resonant lines, but without an engineered cavity are grouped under the term ”random lasers” (RL). There are many examples of RL systems such as: powders of laser crystals [1], dye and scatters in suspension [2], clusters of nanoparticles [3] , films of π-conjugated polymer [4] liquid crystals and dye [5], stacks of slides and dye[6]. Usually random lasing emission spectra are obtained with excitation intensity far above lasing threshold, and thus their spectra contain numerous narrow lines (>20) on top of a broader background of amplified spontaneous emission (ASE); this complicates the analysis of the RL emission spectrum. In spite of this complication

UU IR Author Manuscript

several different theoretical models have been advanced recently that yield a variety of uncorrelated laser lines for explaining the obtained RL spectra [7–10].

In contrast, in this work we look at RL spectra that are obtained just above lasing threshold. We studied RL spectra near threshold excitation in three organic disordered gain systems, namely suspension of dyes and TiO2 scatterers, zinc oxide (ZnO) films, and π-conjugated polymer films. Since there are fewer resonant lines in the emission spectrum near threshold excitation, it allows us to present a more credible analysis of the emission spectrum. Using Fourier transform analysis we found that the RL resonant lines are highly correlated and thus originate from a single resonance structure in each system.

2. EXPERIMENTAL

The basic measurement was the same for the three systems. The excitation was from a Nd:Yag based regenerative amplifier with pulse width of 100 ps and repetition rate ranging from 100 to 800 Hz. The output of the amplifier is either frequency doubled to 532 nm (for the dye and polymer systems), or frequency tripled to 355 nm (for the ZnO system). The emission spectra were collected, focused on the entrance slit of a spectrometer to disperse the spectrum, and then detected with a CCD camera coupled to a computer.

The π-conjugated polymer used here was poly(2,5-dihexyloxy-p-phenylenevinylene) (DHO-PPV) that we synthesized in house [16]. The polymer chain isomerization length determines the solubility, and therefore when choosing a long chain isomerization length and poor solvent, the polymer powder may dissolve, but also form aggregates [15]. The aggregates act as scatterers and both the film and aggregates play an important role in defining the disordered gain medium. The polymer was dissolved in heated toluene, and subsequently allowed to cool down to room temperature. From this solution, a 1 μm thick film was spun cast on a glass substrate. Since the refractive index, n of the polymer at the laser wavelength (n = 1.8) is larger than that of glass (n = 1.4), then the luminescent emission is mostly confined inside the polymer film to form a two-dimensional (2D) disordered gain medium.

The zinc oxide film was made from 100 nm nanoclusters. The nanoclusters were suspended in ethanol and then deposited on a glass substrate. A conglomerate of about 40 microns was used for the measurements. In this case the ZnO nanoparticles are both the gain medium and scatterers.

The dye and scatterers suspension is rhodamine 6G dissolved in ethylene glycol at a concentration of 2 mM, that was mixed with 200 nm diameter TiO2 scatterers at a

UU IR Author Manuscript

concentration of 10^{10} cm^{-3}. The excitation light was focused into a stripe 8 mm long and ~100 micron wide, with the emission collected from the long end of the stripe. The RL emission spectrum contains only a few sharp lines that are well separated. However we note that the spectrum is time dependent, namely it changes dramatically after about 1 millisecond, due to the strong diffusion of scatterers that occurs in the suspension.

3. RESULTS AND DISCUSSION

Random lasing of π-conjugated polymer films has been well studied over the last dozen years [11–13]. Recently spectral mapping of spatial RL emission showed a roughly circular emission region [11, 14]. Here we investigate the emission modes of such system in detail and use the analysis as a prototype for other random lasing systems. The random lasing polymer film has an advantage over other RL systems, since both the gain medium and scatterers are embedded in the same material.

Figure 1 (a) is the RL emission spectrum of the DHO-PPV film excited just above the laser threshold. Typically, the RL emission spectrum contains very narrow lines superposed on a broader ASE background [13]. Since excitation is near threshold, the RL emission spectrum contains a limited number of narrow and well separated peaks. To perform a spectral analysis of Fig. 1 (a) the tool we chose is the power Fourier transform of the emission spectrum [17]. The Fourier transform is usually applied to data that is a time series to try and determine repeating patterns, and resonant frequencies within the data. When applied to an emission spectrum, Fourier transform can reveal the existence of regularities or correlation that exist among the observed peaks. For example, the Fourier transform peak spacing for a linear cavity occurs at nL/π, where n is the index of refraction and L is the separation between the two end mirrors. The polymer film is roughly one wavelength thick and covers a large 2D plane. In a thin polymer film, a linear cavity may not be applicable and some other resonance geometry should be appropriate. The highest symmetry 2D structure is a circle. Previous analysis of fabricated circular microcavities correlated emission laser lines as series of successive integer Bessel functions, Jm [16, 18]. In that analysis, a simplifying approximation was made that the argument of the Bessel function goes to zero at the cavity boundary:

$$Jm(\pi nD/\lambda) = 0, \qquad (1)$$

where D is the circular cavity diameter. The zero condition can be written as $Zm,p = \pi nD/\lambda$, where Zm,p is the pth zero of Bessel function indexed m. Zeros of Bessel functions are numbers that can be calculated with various commercial software packages. In contrast to a

linear cavity, the peak spacing, Δd in the Fourier transform of a 2D circular structure occurs at nD/2, where n is the refraction index. With the product of nD obtained from the Fourier transform of the laser spectrum, the resonant wavelengths can be calculated. Previous coherent backscattering measurements have shown the mean free path in the polymer film to be about 12 μm [19]. This is considered to be a weak scattering regime that is far from Anderson localization, where the scattering length is close to the emission wavelength.

Figure 1 (b) is the power Fourier transform (PFT) of Fig. 1 (a). Typically the units of the Fourier transform are the inverse of the original variable; to have more meaningful results the emission spectrum is first converted to wavenumber ($2\pi/\lambda$) and then transformed. The resulting units are in length and termed pathlength. Our analysis of the laser spectrum is applied to the most intense peak at 634.5 nm. The product of nD/2 that is extracted from Δd in the PFT (Fig. 1 (b)) is 66.7 μm. Plots of higher order Bessel functions, Jn(x), show that maximum intensity is near the first zero of the function. The simplest field structure has a single maximum in the radial function. We start by looking through a table of the first zeros of high index Bessel functions. Bessel function number 644 has the first zero, Z644,1 of 660.1, from which we get using Eq.(1) a resonant emission line at 634.37 nm. The neighboring peaks can be assigned in the same manner. Using the same value of nD allows four major peaks in the spectrum corresponds to successive Bessel functions from Z644,1 (λ = 634.37 nm) to Z647,1 (λ = 631.53 nm). The filled symbols in Fig. 1 (a) show the predicted wavelengths, see inset to Fig. 1 (b). These four peaks have a 0.067 nm RMS difference between measured and calculated values.

There are four more candidate peaks at lower wavelengths that correspond to the next four Bessel functions. Unfortunately, the signal to noise ratio is too small to accurately discern these emission peaks. However our analysis allows eight successive peaks to be assigned with RMS of 0.154 nm (Fig. 1 (b) inset) where the hollow symbols in Fig. 1 (a) show the predicted wavelengths. This assignment procedure has no adjustable parameters, and only assumes a circular resonator. The Bessel function order, m, is selected to be the closest value to the most intense line. We note that with previous fabricated cavities, the analysis worked equally well for a disk or a ring microcavity [16, 18].

Figure 1 (a) and its analysis indicate that all observed peaks in the RL emission spectrum near threshold excitation are in fact correlated to one another, and thus originate from a unique underlying resonance structure in the film. Matching a random lasing spectrum with a circular resonator is surprising. However, there are actually several theoretical works that directly support such a resonance structure. A few works explicitly show that circular rings are

likely resonance structures that can be formed in disordered films [20, 21]. A random media with a disk excitation has been calculated, and its mode structures show the existence of modes at the boundary [22] that may interact stronger than previously anticipated in the polymer film. In coherent backscattering experiments, there is experimental evidence for recurrent multiple scattering, or loops, in strong scattering regimes [23]. We thus infer that in our weakly scattering sample multiple scattering loops might be present, though with a much lower likelihood of occurrence. There is a theoretical work which discuss random lasing films and argues that local regions produce lasing emission [24].

As a random lasing system, there is nothing particularly unique about the π-conjugated polymer. The same analysis can easily be applied to other random lasing systems. Another popular random lasing system is microcrystaline ZnO [3, 25–27]. In this system, micro or nano crystaline ZnO provide both gain medium and scattering mechanism. Fig. 2 (a) shows an SEM micrograph of a conglomerate optically excited with a size roughly 40 μm. Fig. 2 (b) shows the emission spectrum of the entire conglomerate.

The PFT of Fig. 2 (b) is presented in Fig. 2 (c). The highest intensty peak in the emission spectrum occurs at 380.7 nm. Taking the highest intensity PFT harmonic $\Delta l = 21.7\mu m$ gives a value of nD which can be used to calculate an expected peak. The first zero of Bessel function 345 is 368.13 which gives a calculated emission peak of 380.6 nm. Taking the ZnO refraction index of 2.3 gives a diameter of 19 μm. This value fits within the physical size of the conglomerate shown in the picture. As with the polymer film, a series of successive Bessel functions from J351 (λ = 374.1 nm) to J342 (λ = 384.2 nm) matches most of the sharp emission peaks in the RL spectrum. The RMS is 0.18 nm for 10 peaks.

There is a noticeable peak at 381.3 nm which is not within this series. Since the Fourier transform spectrum is more complicated, the next most intense peak PFT harmonic $\Delta l = 13.3$ μm in Fig. 2(c) is used to calculate a second series of emission peaks in ZnO. The same nD value matches the emission peak at 381.2 nm using J_{208}. We note that several emission peaks from both series overlap in the emission spectrum. For example, the observed line at 379.4 nm has predicted peaks in both series at 379.5 predicted value, for both l=21 and l=13. There are 7 possible peaks assigned by this series with an RMS value of 0.40 nm. Actually in the ZnO conglomerate cluster we used there are two circular configurations, and the resulting emission spectrum is a composite of each structure's individual spectrum. The physical size of the conglomerate puts an upper limit on the possible resonator size. We note that both resonator lengths fit within this conglomerate.

UU IR Author Manuscript

To further emphasize the generality of this approach, a third random laser system is investigated. The same analysis can readily be applied to a suspension of TiO2 scatterers in a laser dye [2, 28]. Figure 3 (a) shows the RL emission spectrum from a dye and scatterers suspension pumped just above laser threshold at an intensity of 170 mJ/cm2, that was collected in an interval of 10 miliseconds. The emission peaks seen in Fig. 3 (a) are narrow which again suggests a well confined underlying resonance. Figure 3 (b) is the PFT of Fig.3 (a). There are very distinct peaks which indicate the existence of a strong correlation that may be due to a resonance structure that is transiently formed. The highest symmetry structure in three dimensions is a sphere. The same analysis as above for 2D films is attempted here with the modification that spherical Bessel functions are used: $Jn(x) = (\pi/2x)^{1/2}\ J_{n+1/2}(x)$, where $J_{n+1/2}(x)$ is a regular Bessel function [29]. We look at modes without azimuthal contributions, since they have smallest energy.

This analysis is applied to Fig. 3 (a) by first observing the most intense peak at 562.5 nm. The value nD from the FT in Fig. 3 (b) is 192.6. Looking through a table of the first zeros of high index spherical Bessel functions shows that Bessel function number 1048 has the first zero at a value of 1067.4. Using these values gives a predicted emission peak at 562.4 nm. The neighboring peaks can be assigned in the same manner. Using this nD value allows nine peaks in the spectrum to be assigned to successive spherical Bessel functions, j_{1053} at 559.8 nm to j_{1045} at 564.1 nm. There are additional three peaks that are likely present, but the signal to noise ratio for these is low, and the observed peaks are difficult to ascertain in the emission spectrum. All together, twelve peaks are assigned with a 0.09 nm RMS difference between measured and calculated values. The inset to Fig. 3 (b) shows the difference between measured and calculated peaks wavelengths, the largest difference is 0.18 nm. Not only are all the major peaks determined with this procedure, but even small wiggles that are first overlooked are actually additional resonances.

We now discuss situations where a circular resonance structure can explain unexpected RL spectra. Figure 4 is a RL spectrum from the dye and TiO2 suspension; it is striking because it shows only a single emission line. Nevertheless, we attempt to explain it with an underlying spherical structure. The spectral gain width for rhodamine 6G in solution is about 8 nm. Taking an arbitrary but small size of nD of 20 μm gives spherical Bessel functions j_{103} to match the peak at 566.6 nm. For j_{101} to j_{105} a peak spacing $\Delta\lambda$ for spherical cavities is about 5.2 nm. The inset in 4 shows the rhodamine gain spectrum and next peaks for nD of 20 μm. Only the peak at 566.60 nm has enough gain to overcome losses. If a small spherical resonance structure forms, there would be only a single line which falls within the gain spectrum of the dye, and this explains the RL spectrum having a single resonant line.

UU IR Author Manuscript

4. CONCLUSION

In summary, we presented random lasing spectra from three different organic disordered gain media that were excited just above lasing threshold. Each spectrum contains only few narrow emission lines, in contrast to many such lines that develop at much higher excitation intensity. Using Fourier transform analysis we show that the emission lines are not independent, but are actually highly correlated coming from a simple underlying resonance structure within the gain medium. High symmetry microcavities are in excellent agreement with the RL emission spectra in these systems. When the excited circular or spherical resonance structure crosses lasing threshold, a series of emission modes are produced that correspond to successive Bessel functions. Circular microcavities in 2D and spherical cavities in 3D explain the random lasing quite naturally in these three systems, and thus may be studied more thoroughly to deepen our understanding of RL in disorder gain media.

Acknowledgements
We thank L. Wojchik for the polymer synthesis. This work was supported in part by the DOE under grant No. FG02-04ER46109

References

[1] C. Gouedard, D. Husson, C. Sauteret, F. Auzel, and A. Migus, J. Opt. Soc. Am. B. 10, 2358 (1993).

[2] N. Lawandy, B. R, M, A. Gomes, and E. Sauvain, Nature 368, 436 (1994).

[3] H. Cao, Y. G. Zhao, S. T. Ho, E. W. Seelig, Q. H. Wang, and R. P. H. Chang, Phys. Rev. Lett. 82, 2278 (1999).

[4] S. V. Frolov, Z. V. Vardeny, K. Yoshino, A. Zakhidov, and R. H. Baughman, Phys. Rev. B 59, R5284 (1999).

[5] G. Strangi, S. Ferjani, V. Barna, A. De Luca, C. Versace, N. Scaramuzza, and R. Bartolino, Optics express 14, 7737 (2006).

[6] V. Milner and A. Z. Genack, Phys. Rev. Lett. 94, 073901 (2005).

[7] A. Y. Zyuzin, Phys. Rev. E. 51, 5274 (1995).

[8] X. Jiang and C. M. Soukoulis, Phys. Rev. Lett. 85, 70 (2000).

[9] S. Mujumdar, M. Ricci, R. Torre, and D. S. Wiersma, Phys. Rev. Lett. 93, 053903 (2004).

[10] C. Vanneste, P. Sebbah, and H. Cao, Phys. Rev. Lett. 98, 143902 (2007).

[11] A. Tulek, R. C. Polson, and Z. V. Vardeny, Nature Physics 6, 303 (2010).

[12] R. Polson, M. Raikh, and Z. Vardeny, Selected Topics in Quantum Electronics, IEEE Journal
of 9, 120 (2003), ISSN 1077-260X.

[13] S. Frolov, M. Shkunov, A. Fujii, K. Yoshino, and Z. V. Vardeny, Quantum Electronics, IEEE
Journal of 36, 2 (2000).

[14] R. Polson and Z. V. Vardeny, Optics Letters 35, 2801 (2010).

[15] T.-Q. Nguyen, V. Doan, and B. J. Schwartz, Journal of Chemical Physics 110, 4068 (1999).

[16] R. C. Polson, Z. V. Vardeny, and D. A. Chinn, Applied Physics Letters 81, 1561 (2002),

[17] D. Hofstetter and R. L. Thornton, Applied Physics Letters 72, 404 (1998).

[18] R. C. Polson, G. Levina, and Z. V. Vardeny, Applied Physics Letters 76, 3858 (2000),

[19] R.C. Polson, Z.V. Vardeny ,Physical Review B
71, 045205 (2005)

[20] V. M. Apalkov, M. E. Raikh, and B. Shapiro, J. Opt. Soc. Am. B 21, 132 (2004).

[21] V. M. Apalkov, M. E. Raikh, and B. Shapiro, Phys. Rev. Lett. 89, 016802 (2002).

[22] H. E. Tureci, L. Ge, S. Rotter, and A. D. Stone, Science 320, 643 (2008),

[23] D. S. Wiersma, M. P. van Albada, B. A. van Tiggelen, and A. Lagendijk, Phys. Rev. Lett.

UU IR Author Manuscript

74, 4193 (1995).

[24] R. Frank, A. Lubatsch, and J. Kroha, J. Opt. A: Pure Appl. Opt. 11, 114012 (2009).

[25] R. Thareja and A. Mitra, Applied Physics B(Lasers and Optics) b71, 181 (2000).

[26] Y. Sun, J. Ketterson, and G. Wong, Applied Physics Letters 77, 2322 (2000).

[27] S. Yu, C. Yuen, S. Lau, and H. Lee, Applied Physics Letters 84, 3244 (2004).

[28] W. Sha, C. Liu, and R. Alfano, Optics letters 19, 1922 (1994).

[29] G. B. Afrken and H. J. Weber, Mathematical Methods for Physicists, 5th ed. (Academic Press, 2001).

UU IR Author Manuscript

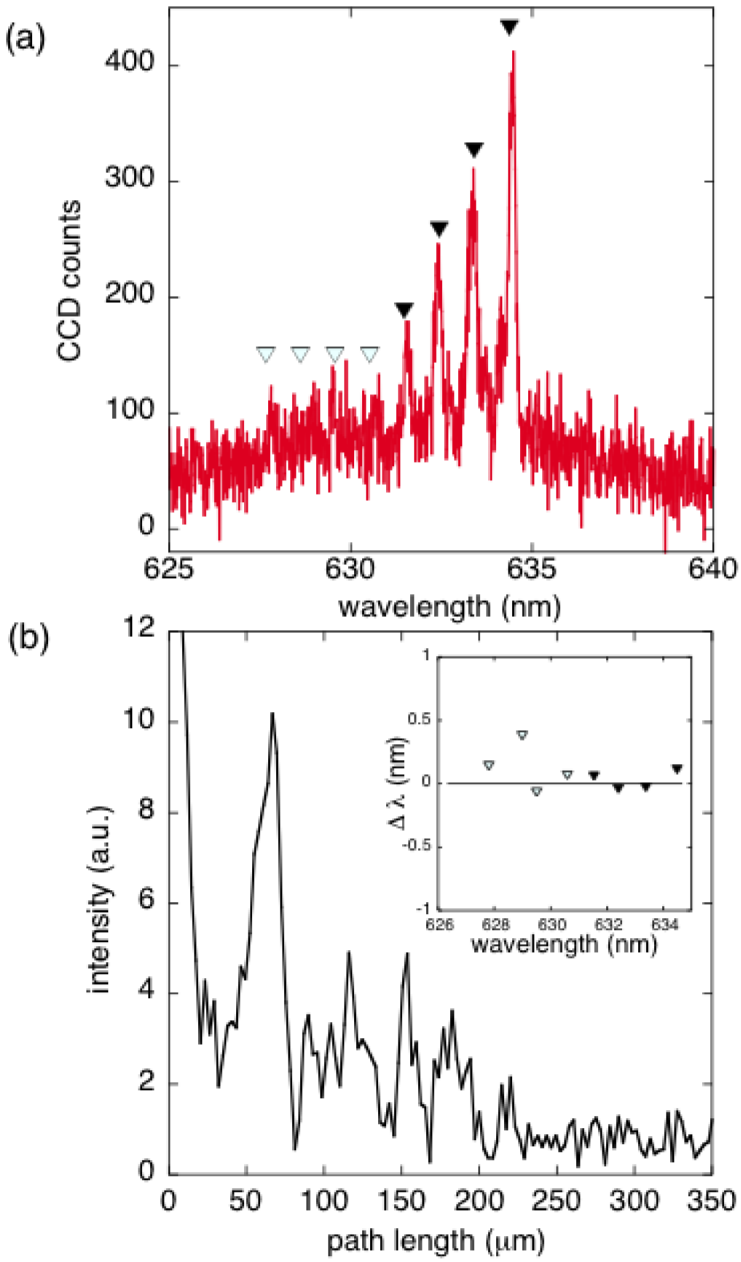

FIG. 1: (Color online) (a) Random laser emission spectrum from a DOOPPV poly- mer film near threshold excitation. (b) Power Fourier transform of (a). (b) inset: Difference between observed and calculated peak positions (see text).

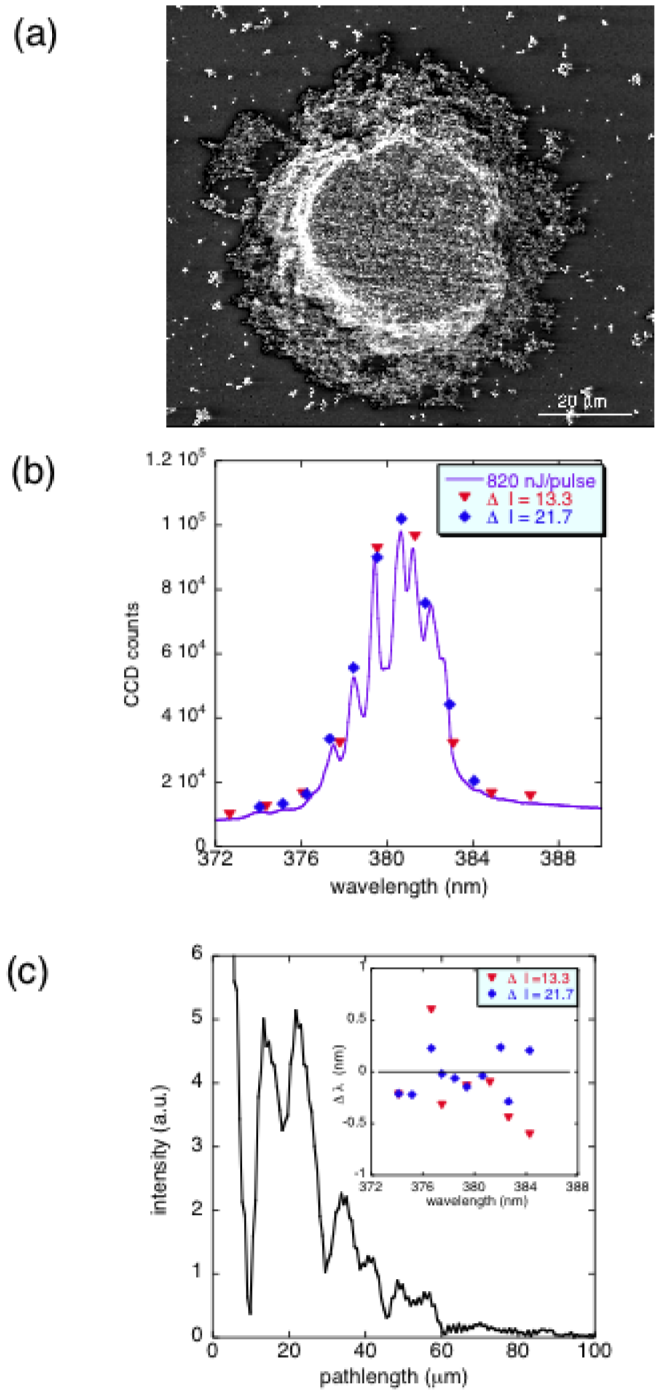

FIG. 2: (a) SEM micrograph of ZnO cluster. (b) Emission spectrum of ZnO cluster pictured in (a). (c) Power Fourier transform of (b).

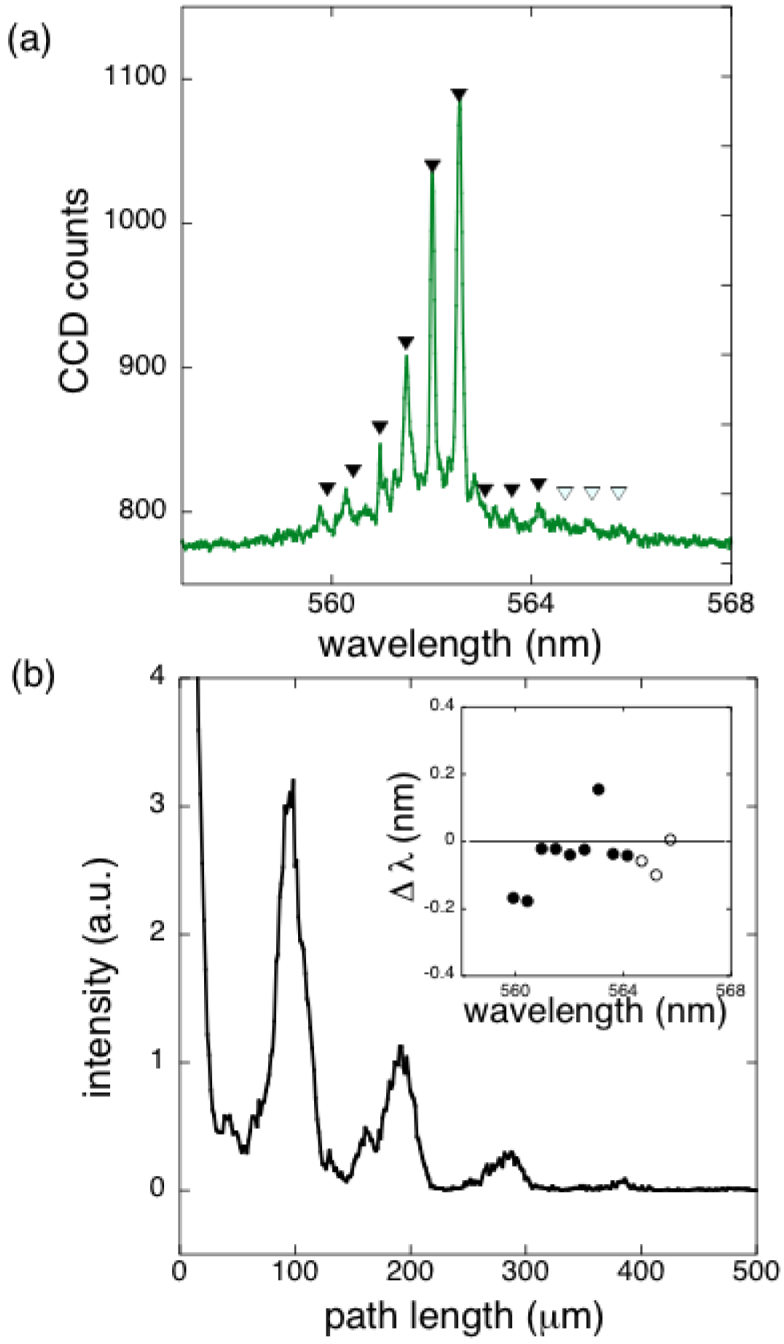

FIG. 3: (Color online) (a) Random laser emission spectrum of rhodamine and TiO2 suspension near threshold. (b) Power Fourier transform of (a). (b) inset: Difference between observed and calculated peak positions.

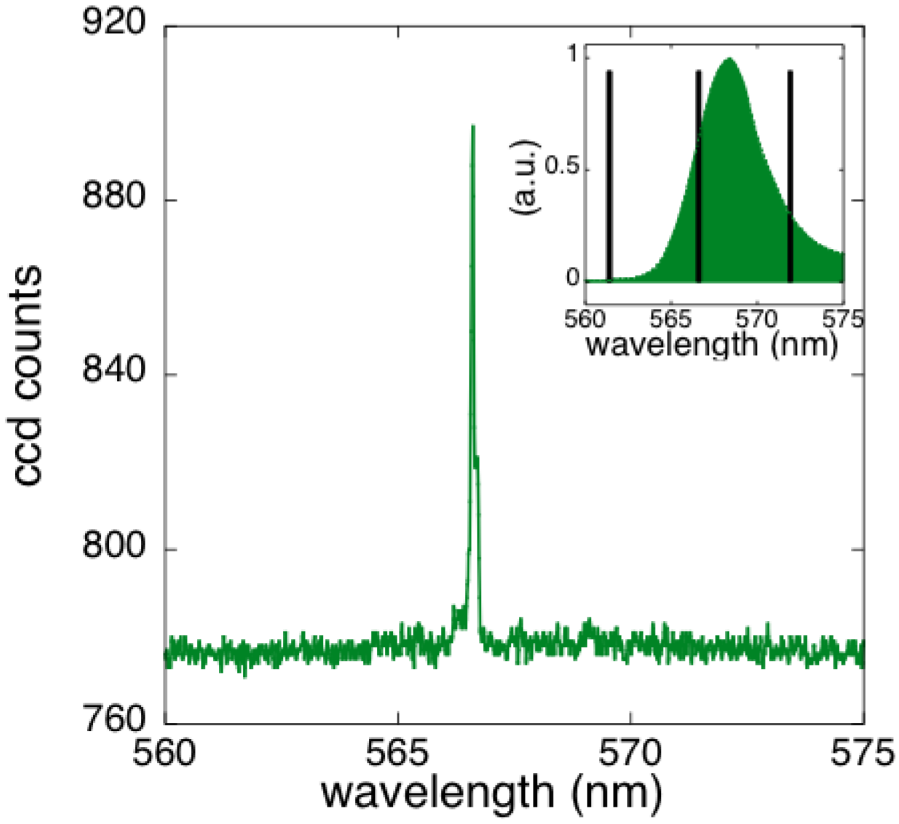

FIG. 4: (Color online) (a) Random lasing in rhodamine 6G dye and TiO2 scatterers that shows a single line. Inset: gain profile of rhodamine 6G and peak spacing for nD=20 µm, (see text).